Supplementary Electronic Information for:

Conformation of the Neurotransmitter γ-Aminobutyric Acid in Liquid Water

Niklas Ottosson[1], Marcin Pastorczak[1,2], Sietse T. van der Post[1], Huib J. Bakker[1]

[1]*FOM Institute AMOLF, Science Park 104, 1098 XG Amsterdam, The Netherlands*
[2]*Present address: Faculty of Physics, University of Warsaw, ul. Hoża 69, 00-681 Warszaw, Poland*

ESI.1 DRS measurements

Dielectric relaxation spectroscopy (DRS) measures the total polarization of the sample, expressed in terms of its complex permittivity $\hat{\varepsilon}(\nu) = \varepsilon'(\nu) - i\varepsilon''(\nu)$. Here ν denotes the field frequency, $\varepsilon'(\nu)$ the in-phase part of the polarization and $\varepsilon''(\nu)$ the out-of-phase, dissipative part. Complex scattering parameters $S_{11}(\nu)$ were obtained in the frequency domain by means of a vector network analyzer (VNA, Rhode-Schwartz model ZVA67). Three different approaches were used to obtain $S_{11}(\nu)$ over the frequency range 10MHz – 90 GHz. At low frequencies (10 MHz – 2 GHz) a cell based on the design of Göttman *et al.* was used,[1] in which the outer coaxial electrode extends several cm from the cable/cell plane, thereby enclosing the liquid sample in the form of a cylindrical column, whereas the inner electrode sticks into the sample as a pin for a distance of 1.8 mm. At intermediate frequencies (500 MHz – 40 GHz) a coaxial disc cell was used, based on the approach by Blackham *et al.*,[2,3] where both the coaxial electrodes are terminated at the sample interface. Finally, at high frequencies (60–90 GHz) a variable-path length waveguide reflection cell was connected to an external frequency converter (Rhode & Schwarz ZVA-Z90E).[4]

A phase-stable coaxial cable (Rhode-Schwartz, ZV-Z96) was connected to the measurement port of the VNA and was calibrated using the accompanying calibration kit (ZV-Z218) employing matched, open and short standards. Further calibration was done upon connecting the respective sample cells in direct connection to measuring the samples. For the two low frequency cells, this was done by measuring scattering parameters for air and pure water

(Milli-Q, ≥18.2 MΩ cm). For the low-frequency pin-cell a 4M NaCl solution was further used to shortcut the cell while conductive silver paint (Pelco, Ted Pella Inc.) was used for shortcutting the intermediate-frequency disc cell. Based on these reference measurements the parameters of a three-term error model[2,3] were obtained for each frequency, moving the calibration plane from the end of the coaxial cable to the probe/sample interface. From the corrected $S_{11}(\nu)$ parameters the complex permittivities of the liquid samples could then be directly calculated.[1,2] In the case of the waveguide cell, calibration at the sample cell interface was made using the WR12 calibration kit from Rhode & Schwartz, providing matched, short and offset-short standards.

ESI.2 Polarization Resolved IR Pump-Probe measurements

ESI.2.1 Preparation of isotopically diluted samples

For the fs-IR experiments we prepared solutions of various concentrations of γ-amino butyric acid (GABA, >99% purity, Sigma Aldrich) in isotopically diluted water (5% (w/w) of D_2O and 95% (w/w) of H_2O). The D_2O (Aldrich) contained over 99.99 % of D atoms and the H_2O was purified with the use of a MiliQ system (Millipore). The solvent was isotopically diluted in order to suppress ultrafast resonant vibrational energy hopping known as Förster energy transfer.[5] The isoelectric point of GABA is pI = 7.3 and when dissolved in water it primarily exists in its zwitterionic form. The cationic form of GABA was obtained by the addition of perchloric acid (ACS reagent 70% aqueous solution, Sigma Aldrich). We chose this acid since the OD groups of HDO molecules solvating perchlorate anions have their vibrational stretching resonance shifted from 2500 cm^{-1} to 2640 cm^{-1}.[6] The contribution of these OD groups to the pump-probe response can therefore be distinguished from the response of the OD groups forming hydrogen bonds to other water molecules or to cationic GABA. The pH of the acidic solutions was prepared to be 1.8 ± 0.2. At this pH, 99.6% of the GABA molecules are in their cationic form (calculated with CurTiPot[7] software).

For the spectroscopic measurements the samples were placed between two CaF_2 windows (4 mm thickness) with a 25 μm Teflon spacer in between. Steady-state spectra of the solutions were measured with an FTIR spectrometer (Bio-Rad).

ESI.2.2 Experimental details

The mid-infrared femtosecond laser pulses were obtained in a number of conversion steps using the output of a Ti:Sapphire laser (Hurricane, Spectra-Physics). The Ti-Sapphire laser

generates linearly polarized 800 nm pulses with a duration of 110 fs and a pulse energy of 0.9 mJ. Part of the light (60%) was used to pump an Optical Parametric Amplifier (OPA, Spectra-Physics) that down converts the pulses to 2000 nm in a beta-barium borate (BBO) crystal. These pulses were frequency-doubled in a second BBO crystal. The 1000 nm pulses thus obtained were combined with the remaining 40% of the 800 nm Ti:Sapphire output to produce 4000 nm pulses via difference-frequency generation in a $LiNbO_3$ crystal.

Most energy of the 4000 nm (2500 cm^{-1}) pulses (4 μJ) was used to excite the OD stretch vibration of a fraction of the HDO molecules to their first excited state. This excitation leads to two absorption changes: (1) a decreased absorption (bleaching) at the fundamental $0\rightarrow1$ transition frequency due to the depletion of the ground state and $1\rightarrow0$ stimulated emission and (2) an increased absorption at the $1\rightarrow2$ transition frequency. This induced absorption is anharmonically blue-shifted from the fundamental transition by 180 cm^{-1}. We probed the absorption changes with a weak (200 nJ) pulse that is delayed from the pump pulse by a delay time t. The polarization of the probe pulses is rotated 45° with respect to the polarization of the pump pulses. A wire grid polarizer located behind the sample reflects the polarization component oriented parallel and transmits the polarization component that is oriented perpendicular with respect to the pump polarization. This configuration enables us to measure the absorption changes in both polarization directions simultaneously on two different array lines of a Mercury-Cadmium-Telluride (MCT) array detector. Every second pump pulse was blocked by a 500 Hz chopper to obtain both the pumped and the unpumped absorption spectra, from which we obtained the transient absorption difference spectra $\Delta\alpha_{\parallel}$ and $\Delta\alpha_{\perp}$. With these two signals, we construct the isotropic signal $\Delta\alpha_{iso}$ that only contains information about the vibrational lifetime of the OD oscillators:

$$\Delta\alpha_{iso}(\omega,t) = \frac{\Delta\alpha_{\parallel}(\omega,t) + 2\Delta\alpha_{\perp}(\omega,t)}{3} \qquad \text{(ESI.1)}$$

The linearly polarized pump pulse preferentially excites OD oscillators that are oriented parallel to the pump polarization. The anisotropy of the distribution of excited OD oscillators leads to a difference between the absorption changes that are probed parallel and perpendicular, which decays in time due to molecular reorientation. The anisotropy parameter $R(\omega,\tau)$ exclusively represents the molecular reorientation of the OD groups and is written as the normalized difference between $\Delta\alpha_{\parallel}$ and $\Delta\alpha_{\perp}$:

$$R(\omega, t) = \frac{\Delta\alpha_{\parallel}(\omega, t) - \Delta\alpha_{\perp}(\omega, t)}{\Delta\alpha_{\parallel}(\omega, t) + 2\Delta\alpha_{\perp}(\omega, t)} \qquad \text{(ESI.2)}$$

Note that the contribution of the vibrational relaxation thereby is divided out in $R(\omega, t)$.

ESI.1.3 Auxiliary measurements

Upon preparation, all samples were measured using a densitometer (LiquiPhysics Excellence DM40, Mettler Toledo). This measurement allows the conversion between the sample solute molal (m) and molar (M) concentration scales, and allows for a precise calculation of the water concentration in all samples. Furthermore, the pH measurements of all samples was measured using a calibrated S20 Seven Easy pH meter (Mettler Toledo).

ESI.3 Modeling of the fs-IR transient spectra

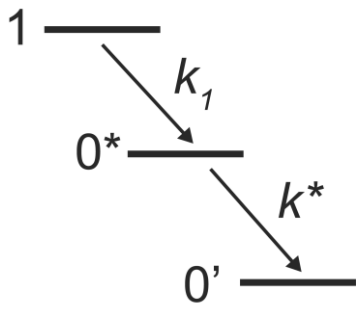

Scheme ESI.1) *Schematic representation of the kinetic model for vibrational relaxation described in the text. k_1 represents the decay rate of the excited state to the intermediate state (starred). The population in the intermediate state decays to the thermalized ground state (accented) with decay rate k*.*

Fig. ESI.1 shows the isotropic transient absorption spectra that were obtained for various pump-probe delay times in a solution of 4m GABA, dissolved in isotopically diluted water. At short delay times there is a bleaching signal that decays within a few picoseconds. The signal that remains constant for delay times as long as 100 ps results from a heating of the sample due to the energy dissipation of the absorbed pump pulse after vibrational relaxation

[S1]. Heating of water leads to a weakening of the hydrogen bonds, which in turn induces a blue-shift of the OD stretch frequency. Hence, the heating of the sample manifests itself in the pump-probe signal as a bleaching signal in the red wing of the absorption band and an induced absorption in the blue wing of the absorption band. In order to calculate the anisotropy of the excited OD oscillators, we need to subtract the heating contribution from the transient spectra at all delay times. To do so, we obtain the population dynamics of the thermalized state by fitting a kinetic model for vibrational decay to the isotropic data. It has been observed experimentally that the rise of the heating signal is delayed with respect to the decay of the excited state.[8] Hence, we use a kinetic model in which the excited OD stretch vibration first relaxes to an intermediate state with time constant $t_1=1/k_1$. This intermediate state subsequently relaxes to the heated ground state with time constant $t^*=1/k^*$ (see Scheme S1). The delayed rise of the heating effect likely results from the relatively slow adaptation of the water hydrogen-bond network to the higher energy content of the low-energy degrees of freedom, resulting from the relaxation of the excited OD stretch vibration. Therefore, the transient absorption spectrum of the intermediate state has no spectral signature in the measured spectral range, meaning that the absorption spectrum of this state closely resembles that of the ground state. The solid lines in Fig. ESI.1 represent the results of the fit.

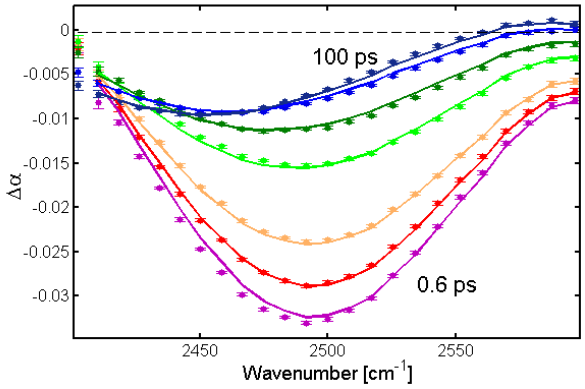

Fig. ESI. 1) *Transient absorption spectra measured for a solution of 4 m GABA in 10% HDO–H_2O for pump–probe delay times of 0.6, 0.8, 1.2, 2, 3, 5 and 100 ps. The solid lines represent the fit to the model described in the text.*

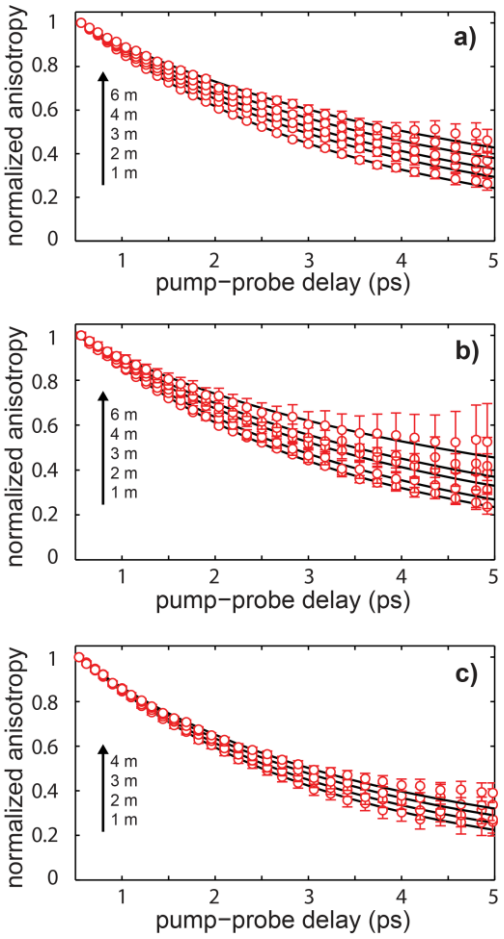

Figure ESI.2) *OD-stretch anisotropy decays of a) 1-6 m GABA solutions at neutral pH (predominantly zwitterions), b) 1-6 m L-proline solutions at neutral pH (predominantly zwitterions), and c) 1-4 m GABA solutions at pH = 1.8 ± 0.2 (predominantly cationic GABA).*

For all delay times, we subtract the heat contribution from the measured $\Delta\alpha_{\parallel}$ and $\Delta\alpha_{\perp}$. The thus corrected signals were used to construct the anisotropy dynamics according to Equation S2. The results obtained for different concentrations of GABA and L-proline are shown in Fig. ESI.2 (together with the results of the fits to the model discussed in section ESI.4). Since the anisotropy dynamics show no frequency dependence between 2480 – 2520 cm^{-1}, we averaged the values of R in this frequency range.

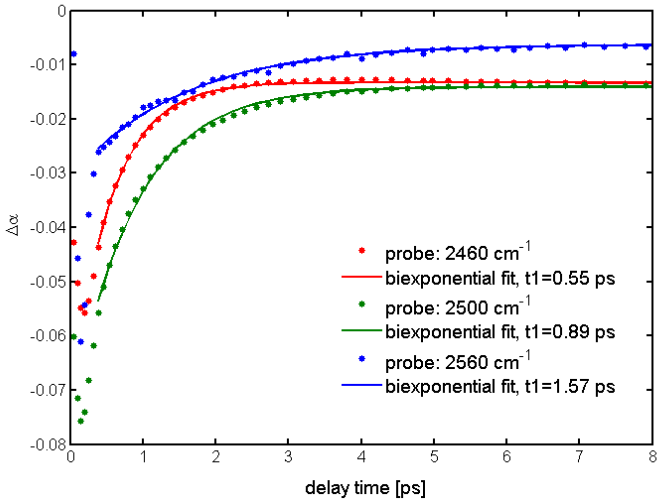

Figure ESI.3) *Isotropic pump-probe signal traces, $\Delta\alpha_{iso}(\omega, t)$, as a function of delay time at three different frequencies: 2460 cm^{-1} (red), 2500 cm^{-1} (green) and 2560 cm^{-1} (blue). The solid lines represent biexponential fits to experimental data.*

The kinetic model shown in Scheme ESI.1 was used to model the results obtained for zwitterionic GABA (at neutral pH) and L-proline solutions. The results obtained for the charged solutions of GABA contains an additional contribution, so the model needs to be extended. For the time-resolved experiment on acidic solutions of GABA, we centered the pump pulse around 2460 cm^{-1} in order to minimize the excitation of the OD groups hydrating perchlorate (see further the section on sample preparation). Figure ESI.3 shows a number of delay traces that were obtained for a 4m GABA solution at pH = 1.8. The bleaching signal at 2560 cm^{-1} shows a decay with a relaxation time of T_1= 1.57 ps, similar to the value that was obtained for neat HDO/H_2O (1.7±0.1 ps).[9] The vibrational relaxation of perchlorate bound OD groups was estimated by Gaffney to be 5 ps.[10] We may thus conclude that we do not observe any contribution of OD groups associated with perchlorate in the measured spectral window. The same graph shows delay traces at lower frequencies, from which it is clear that the relaxation on the red side of the spectrum is faster than on the blue side (T_1=0.89 ps at 2500 cm^{-1} and T_1=0.55 ps at 2460 cm^{-1}). This frequency dependence of t_1 is modeled by assuming two excited states that both decay by different channels: a fast channel at the red side and a slow channel at the blue side of the spectrum (the kinetic model is depicted in Scheme ESI.2). The fast relaxation channel can be assigned to response of a broad absorption associated with Eigen and Zundel proton hydration complexes.[11]

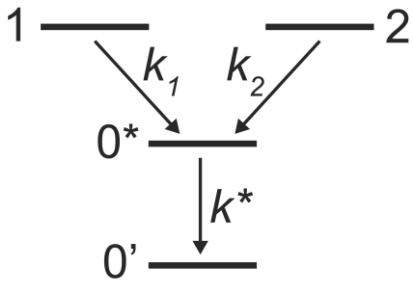

Scheme ESI.2: Schematic representation of the kinetic model for vibrational relaxation in solutions of GABA at low pH. There are two excited states that decay with different rates to the intermediate state.

ESI.4 Combined modeling of experimental data

For multi-component dipolar liquids several dispersion steps in $\hat{\varepsilon}(\nu)$ can typically be observed, one pertaining to each relaxation process.[12] In pure water, two distinct Debye processes have been identified: The main process (τ_{bulk}=8.4 ps) is related to the cooperative relaxation of the hydrogen bond network[13,14] while the nature of the weak high-frequency process (τ_{fast}=1.1 ps) has been the subject of some debate.[15,16] Due to the small contribution of the fast water process in the frequency window probed we do not include this mode in our fitting model. In addition to the main bulk water reorientation process, we observe the dielectric relaxation of the solutes and of a sub-ensemble of water molecules that are slowed down compared to bulk water, as a result of their interaction with the solute. We find that for all measured samples the frequency-dependent complex dielectric function can be fitted well to a relaxation model consisting of three Debye modes and a conductivity term, i.e.

$$\hat{\varepsilon}(\nu) = \frac{S_{solute}}{1 + i2\pi\nu\tau_{solute}} + \frac{S_{slow}}{1 + i2\pi\nu\tau_{slow}} + \frac{S_{bulk}}{1 + i2\pi\nu\tau_{bulk}} + \frac{i\sigma}{\varepsilon_0 2\pi\nu} + \varepsilon_\infty \qquad \text{(ESI.3)}$$

in which S_{solute}, S_{slow} and S_{bulk} denote the dielectric strengths of the modes pertaining to the solute (low frequencies, $\tau_{sol.}$= 50-400 ps), slow water (intermediate frequencies, τ_{slow}= 30-40 ps) water and bulk water (high frequencies, τ_{bulk}= 8.4 ps), respectively. ε_∞, or the "infinite" permittivity, gives the in-phase response in the high frequency limit at which the orientational contributions from the three Debye modes have vanished. The loss terms $i\sigma/\varepsilon_0 2\pi\nu$, arising due to the conductivity σ of the electrolyte, have been subtracted from the spectra shown in the main manuscript for visual clarity.

As discussed in the main text, the solute relation times can be well fitted to the functional form $\log(\tau_{\mathrm{solute}}) = \mathrm{A} \times \mathrm{X}_{\mathrm{solute}} + \mathrm{B}$. The thus extracted parameters A and B are given in Table ESI.1 for aqueous solutions of zwitterionic and cationic GABA, as well as zwitterionic L-proline.

Table ESI.1) *Extracted fit parameters on the form* $log(\tau_{solute}) = A \times X_{solute} + B$ *for all solutions, as plotted in Fig. 4 of the main text.*

	A	B
Zwitterionic $GABA_{aq}$	6.47	1.95
Cationic $GABA_{aq}$	3.20	1.93
Zwitterionic L-proline	6.10	1.72

The amplitudes $\mathrm{S}_{\mathrm{slow}}$ and $\mathrm{S}_{\mathrm{bulk}}$ of the two water modes are related to the expected total dielectric strength $\mathrm{S}_{\mathrm{H2O,tot}}$ from each sample's water concentration via the relation $\mathrm{S}_{\mathrm{bulk}} = \mathrm{S}_{\mathrm{H2O,tot}} - \mathrm{S}_{\mathrm{slow}} - \mathrm{S}_{\mathrm{IB}} - \mathrm{S}_{\mathrm{KD}}$.[17] Here S_{IB} gives the depolarization due to irrotational binding of water dipoles due to the solutes (primarily due to the cationic ammonium groups), which is thus assumed to remove spectral intensity merely from the bulk water DR mode. S_{KD} only arises in conducting samples (which in the current study only applies to the acidic solutions of cationic GABA), due to the coupling of the translational motion of the ionic solute to the rotational motion of the solvent. This contribution can be calculated from the theory of Hubbard and Onsager[18-20] as

$$\mathrm{S}_{\mathrm{KD}} = \sigma \frac{2}{3} \frac{\varepsilon_{\mathrm{S}}(0) - \varepsilon_{\infty}(\mathrm{c})}{\varepsilon_{\mathrm{S}}(0)} \frac{\tau_{\mathrm{D}}(0)}{\varepsilon_0} \qquad \text{(ESI.4)}$$

where σ is the dc conductivity of the solutions, $\varepsilon_{\mathrm{S}}(0)$ refers to the dielectric constant of the pure solvent, $\varepsilon_{\infty}(\mathrm{c})$ is the infinite permittivity of the solution of concentration c, $\tau_{\mathrm{D}}(0)$ is the Debye relaxation time of the pure solvent and ε_0 is the vacuum permittivity.

In order to relate the dielectric strength S_j of the *j*:th mode in the permittivity spectrum to the concentration c of the contributing dipoles, each having an effective dipole moment μ_{eff}, we have used the Cavell equation[21];

$$S_j = \frac{\varepsilon_S}{2\varepsilon_S + 1}\frac{N_A c}{k_B T \varepsilon_0} \cdot \mu_{eff}^2 \qquad \text{(ESI.5)}$$

where ε_S is the solution's dielectric constant and ε_0 is the vacuum permittivity.

The decay of the anisotropy of the water O-D stretch in the time-domain, as obtained from our fs-mid-IR experiments, is well fitted by the bi-exponential function

$$R(t) = A_1 \cdot e^{-\xi \cdot t/\tau_{slow}} + A_2 \cdot e^{-\xi \cdot t/\tau_{bulk}} \qquad \text{(ESI.6)}$$

in which ξ = 3.4 gives the ratio between the Debye and second-order relaxation time constants of the dipolar/O-H auto-correlation functions, as measured in the DRS and fs-mid-IR experiments, respectively.[22,23] Hence, the extracted reorientation time constants for the slow and bulk water are simultaneously constrained by the data obtained with both techniques. Furthermore, the relative fitted amplitude of the two water components in Eq. 2 is linked to the DRS data via $A_2/A_1 = (S_{H2O,tot} - S_{slow})/S_{slow}$.

For all solutions, S_{KD} was calculated from the measured conductivity while $S_{H2O,tot}$ computed calculated from the Cavell equation using the analytic water concentrations obtained from density measurements. While fitting S_{bulk} and S_{slow} to the permittivity spectra in conjunction to the fs-IR data we hence obtain the value S_{IB} that is missing from the expected dielectric response of water. Using the Cavell equation, S_{IB} can in turn be translated into a water concentration c_{IB} from which we calculate the concentration dependent dynamical coordination number as;

$$Z_{IB} = \frac{c_{IB}}{c} \qquad \text{(ESI.7)}$$

Where c denotes the concentration of the solute.

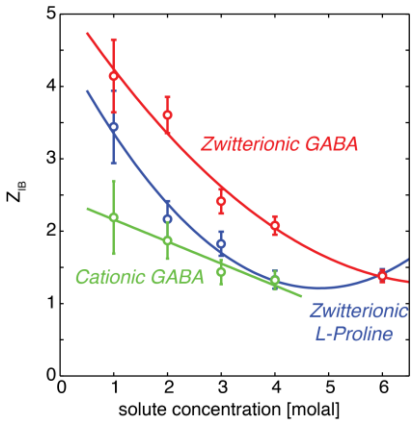

Figure ESI.4) *Hydration number Z_{IB} for zwitterionic (red) and cationic (green) GABA in aqueous solution as a function of concentration. The data points are extracted from the fit to the dielectric data using Eq. ESI.3. The lines are mere guides to the eye from a second order polynomial fit.*

Z_{IB} is plotted in Fig. ESI.4 for all solutions discussed in the main text. The values are overall similar to those found in previous studies of aqueous amino acids[24,25], and show a moderate decrease with increasing concentration.

From the simultaneous fits of the water response in the fs-IR and DRS data we obtain the first order dipolar reorientation time constant of the slow water ensemble; this parameter is given in Fig. ESI.5a, as a function of the total water molar fraction. As is commonly observed, and discussed in the main text, we see that the overall solution dynamics is slowed down at higher solute concentrations (smaller water fractions). Using the Cavell equation we can relate the amplitude S_{slow} to the concentration c_{slow} of slow water molecules in the sample. Analogous to the irrotational binding number Z_{IB} we thus obtain a slow (hydrophobic) hydration number Z_S as:

$$Z_S = \frac{c_{slow}}{c} \qquad \text{(ESI.8)}$$

which is given in panel b) of Fig. ESI.5 for all investigated samples. As previously observed in the hydration of carboxylate anions,[26] this parameter shows a significant concentration dependence.

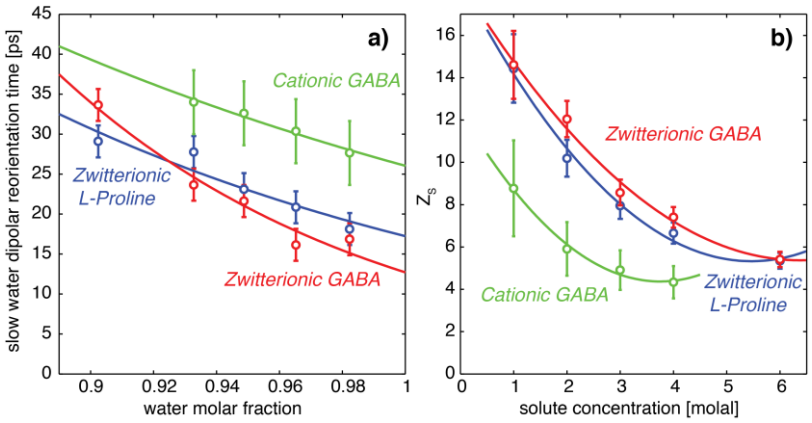

Figure ESI.5) *Panel a) gives the time constant τ_{slow} of the slow water fraction for the three types of solutions investigated. The open circular markers were obtained from a fit to Eq. ESI.3 of the respective permittivity spectra. The lines in panel a) are in term fits of the form $log(\tau_{slow}) = A \times X_{water} + B$. Panel b) gives the associated hydrophobic hydration number Z_S. The lines are guides to the eye.*

ESI References

1. Göttmann, O., Kaatze, U. & Petong, P. Coaxial to circular waveguide transition as high-precision easy-to-handle measuring cell for the broad band dielectric spectrometry of liquids. *Measurement Science and Technology* **7**, 525 (1996).
2. Blackham, D. V. & Pollard, R. D. An improved technique for permittivity measurements using a coaxial probe. *Instrumentation and Measurement, IEEE Transactions on* **46**, 1093-1099 (1997).
3. Ensing, W., Hunger, J., Ottosson, N. & Bakker, H. J. On the Orientational Mobility of Water Molecules in Proton and Sodium Terminated Nafion Membranes. *J. Phys. Chem. C* **117**, 12930-12935 (2013).
4. Hunger, J., Cerjak, I., Schoenmaker, H., Bonn, M. & Bakker, H. J. Precision waveguide system for measurement of complex permittivity of liquids at frequencies from 60 to 90 GHz. *Rev. Sci. Instrum.* **82**, 104703 (2011).
5. Piatkowski, L., Eisenthal, K. B. & Bakker, H. J. Ultrafast intermolecular energy transfer in heavy water. *Phys. Chem. Chem. Phys.* **11**, 9033-9038 (2009).
6. Bergström, P. Å., Lindgren, J. & Kristiansson, O. An IR study of the hydration of perchlorate, nitrate, iodide, bromide, chloride and sulfate anions in aqueous solution. *J. Phys. Chem.* **95**, 8575-8580 (1991).
7. CurTiPot - pH and Acid–Base Titration Curves: Analysis and Simulation software version 3.6.1 (2012).
8. Lock, A. J., Woutersen, S. & Bakker, H. J. Ultrafast Energy Equilibration in Hydrogen-Bonded Liquids. *J. Phys. Chem. A* **105**, 1238-1243 (2001).
9. Rezus, Y. L. A. & Bakker, H. J. On the orientational relaxation of HDO in liquid water. *J. Chem. Phys.* **123**, 114502 (2005).
10. Ji, M. & Gaffney, K. J. Orientational relaxation dynamics in aqueous ionic solution: Polarization-selective two-dimensional infrared study of angular jump-exchange dynamics in aqueous 6M NaClO4. *J. Chem. Phys.* **134**, 044516 (2011).
11. Woutersen, S. & Bakker, H. J. Ultrafast Vibrational and Structural Dynamics of the Proton in Liquid Water. *Phys. Rev. Lett.* **96**, 138305 (2006).
12. Kremer, F. & Schönhals, A. *Broadband Dielectric Spectroscopy*. (Springer Verlag, Berlin, Heidelberg, New York, 2002).
13. Buchner, R., Barthel, J. & Stauber, J. The dielectric relaxation of water between 0 °C and 35 °C. *Chem. Phys. Lett.* **306**, 57-63 (1999).
14. Fukasawa, T. *et al.* Relation between Dielectric and Low-Frequency Raman Spectra of Hydrogen-Bond Liquids. *Phys. Rev. Lett.* **95**, 197802 (2005).
15. Yada, H., Nagai, M. & Tanaka, K. Origin of the fast relaxation component of water and heavy water revealed by terahertz time-domain attenuated total reflection spectroscopy. *Chem. Phys. Lett.* **464**, 166-170 (2008).
16. Zasetsky, A. Y. Dielectric Relaxation in Liquid Water: Two Fractions or Two Dynamics? *Phys. Rev. Lett.* **107**, 117601 (2011).
17. We are thereby assuming that the effective dipole moment of water molecules in the solutions as the same as in pure water.
18. Hubbard, J., Onsager, L., Beek, W. M. v. & Mandel, M. Kinetic polarization deficiency in electrolyte solutions. *Proc. Nat. Ac. Sci.* **74**, 401 (1977).
19. Hubbard, J. & Onsager, L. Dielectric dispersion and dielectric friction in electrolyte solutions. I. *J. Chem. Phys.* **67**, 4850 (1977).
20. Buchner, R., Hefter, G. T. & May, P. M. Dielectric Relaxation of Aqueous NaCl Solutions. *J. Phys. Chem. A* **103**, 1-9 (1999).
21. Cavell, E. A. S., Knight, P. C. & Sheikh, M. A. Dielectric relaxation in non aqueous solutions. Part 2.—Solutions of tri(n-butyl)ammonium picrate and iodide in polar solvents. *Trans. Faraday Soc.* **67**, 2225-2233 (1971).

22. Laage, D. & Hynes, J. T. A Molecular Jump Mechanism of Water Reorientation. *Science* **311**, 832-835 (2006).
23. Tielrooij, K. J., Petersen, C., Rezus, Y. L. A. & Bakker, H. J. Reorientation of HDO in liquid H_2O at different temperatures: Comparison of first and second order correlation functions. *Chem. Phys. Lett.* **471**, 71-74 (2009).
24. Sato, T., Buchner, R., Fernandez, S., Chiba, A. & Kunz, W. Dielectric relaxation spectroscopy of aqueous amino acid solutions: dynamics and interactions in aqueous glycine. *J. Mol. Liq.* **117**, 93-98 (2005).
25. Rodriguez-Arteche, I., Cerveny, S., Alegria, A. & Colmenero, J. Dielectric spectroscopy in the GHz region on fully hydrated zwitterionic amino acids. *Phys. Chem. Chem. Phys.* **14**, 11352-11362 (2012).
26. Rahman, H. M. A., Hefter, G. & Buchner, R. Hydrophilic and Hydrophobic Hydration of Sodium Propanoate and Sodium Butanoate in Aqueous Solution. *J. Phys. Chem. B* **117**, 2142-2152 (2013).